A Domain Decomposition Method for Large Scale Simulations of Two-phase Flows with Moving Contact Lines

Li Luo[1], Qian Zhang[1], Xiao-Ping Wang[1], Xiao-Chuan Cai[2]

[1]Department of Mathematics,
The Hong Kong University of Science and Technology, Hong Kong

[2]Department of Computer Science,
University of Colorado Boulder, Boulder, USA

DD23
July 8, 2015
Jeju Island, Korea

Outline

Outline

Outline

Outline

Outline

Outline

Outline

Outline

Background of two-phase flow

Liquid-vapor interface

Liquid-liquid interface

Moving contact line problems

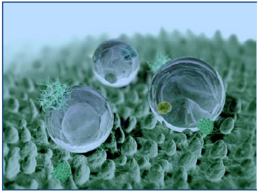

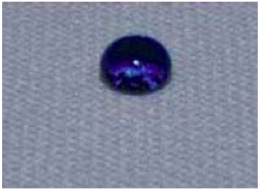

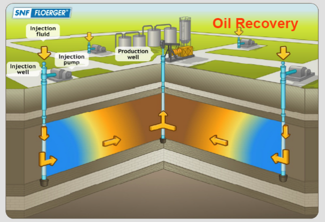

When the fluid-fluid interface intersects the solid wall, it creates a moving contact line.

Phase-field

Consider two different fluids with densities ρ_1 and ρ_2. Define the phase-field

$$\phi(x) = \frac{\rho_1 - \rho_2}{\rho_1 + \rho_2} = \begin{cases} 1, & \text{for fluid 1} \\ 0, & \text{at interface} \\ -1, & \text{for fluid 2} \end{cases}$$

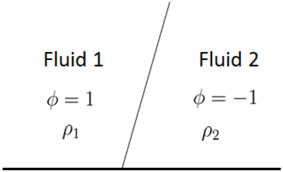

Cahn-Hilliard Theory

Free energy functional:

$$\mathcal{F}_\Omega(\phi) = \int_\Omega [\frac{1}{2}\epsilon(\nabla\phi)^2 + \frac{1}{\epsilon} f(\phi)]\mathrm{d}\Omega,$$

$$f(\phi) = -\frac{1}{2}\phi^2 + \frac{1}{4}\phi^4$$

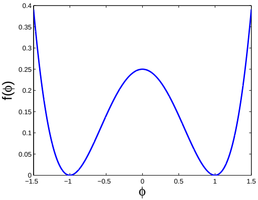

Equilibrium in 1D:

$$\epsilon\phi_{zz} + \frac{1}{\epsilon}(\phi - \phi^3) = 0,$$

$$\phi(z) = \tanh\left(\frac{z}{\sqrt{2}\epsilon}\right)$$

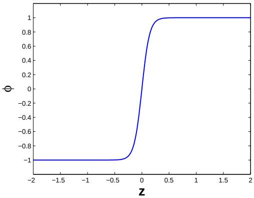

Outline

Model

A coupled Cahn-Hilliard and Navier-Stokes system is used to model the MCL problem, as follows:

$$\frac{\partial \phi}{\partial t} + \mathbf{v} \cdot \nabla \phi = \mathcal{L}_d \Delta \mu, \qquad in \quad \Omega, \tag{2.1}$$

$$\mathrm{Re}\rho[\frac{\partial \mathbf{u}}{\partial t} + (\mathbf{u} \cdot \nabla)\mathbf{u}] = -\nabla p + \nabla \cdot [\eta D(\mathbf{u})] + \mathcal{B}\mu\nabla\phi, \qquad in \quad \Omega, \tag{2.2}$$

$$\nabla \cdot \mathbf{u} = 0, \qquad in \quad \Omega. \tag{2.3}$$

Here $\mu = -\epsilon\Delta\phi - \phi/\epsilon + \phi^3/\epsilon$ is the chemical potential, ϵ is the ratio between interface thickness ξ and characteristic length L; density $\rho = \frac{1+\phi}{2} + \lambda_\rho \frac{1-\phi}{2}$, viscosity $\eta = \frac{1+\phi}{2} + \lambda_\eta \frac{1-\phi}{2}$, $\lambda_\rho = \rho_2/\rho_1$ and $\lambda_\eta = \eta_2/\eta_1$ are density and viscosity ratios; $\mathbf{u} = (u_x, u_y, u_z)$ where u_x, u_y, u_z are velocities along x, y, z directions, $D(\mathbf{u}) = \nabla\mathbf{u} + (\nabla\mathbf{u})^T$ is the rate of stress tensor.

Model

The motion of the contact line at solid boundaries can be described by the generalized Navier boundary condition (GNBC) [Qian et. al, 03, 06] which evaluates the velocity as:

$$[\mathcal{L}_s l_s]^{-1} u_{\tau_1}^{slip} = \mathcal{B}L(\phi)\partial_{\tau_1}\phi/\eta - \mathbf{n}\cdot D(\mathbf{u})\cdot\tau_1, \tag{2.4}$$

$$[\mathcal{L}_s l_s]^{-1} u_{\tau_2}^{slip} = \mathcal{B}L(\phi)\partial_{\tau_2}\phi/\eta - \mathbf{n}\cdot D(\mathbf{u})\cdot\tau_2, \tag{2.5}$$

here $L(\phi) = \epsilon\partial_n\phi + \partial\gamma_{wf}(\phi)/\partial\phi$, and $\gamma_{wf}(\phi) = -\frac{\sqrt{2}}{3}\cos\theta_s^{surf}\sin(\frac{\pi}{2}\phi)$; slip length $l_s = \frac{1+\phi}{2} + \lambda_{l_s}\frac{1-\phi}{2}$. τ_1 and τ_2 are two unit tangent directions along the solid surface, $\tau_1\cdot\tau_2 = 0$.

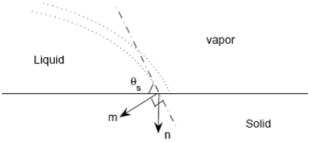

In addition, a relaxation boundary condition is imposed on the phase function

$$\frac{\partial\phi}{\partial t} + u_{\tau_1}\partial_{\tau_1}\phi + u_{\tau_2}\partial_{\tau_2}\phi = -\mathcal{V}_s[L(\phi)], \tag{2.6}$$

together with the following impermeability conditions:

$$u_n = 0, \quad \partial_n\mu = 0. \tag{2.7}$$

Outline

Discretization

1. Discretization in time: a semi-implicit scheme
   - Cahn-Hilliard equaiton: nonlinear terms and high order derivative impose severe constrains on time step length and difficulties for finite-element discretizations
     — Separate into two equations of ϕ and μ
     — Convex splitting method [Eyre, 98]
   - Navier-Stokes equations: variable density as a coefficient
     — A pressure stabilized scheme [Gao and Wang, 12] further decouples the velocity and pressure
     — A pressure Poisson equation is to be solved

2. Discretization in space: a piecewise linear continuous finite element method

$$W_h = \{w_h \in C^0(\overline{\Omega}) \cap H^1(\Omega) : w_h|_T \in P_1(T) \text{ or } Q_1(T), \forall T \in \mathcal{T}_h\},$$
$$\mathbf{U}_h = \{\mathbf{u}_h \in [C^0(\overline{\Omega}) \cap H_0^1(\Omega)]^3 : \mathbf{u}_h|_T \in P_1(T)^3 \text{ or } Q_1(T)^3, \forall T \in \mathcal{T}_h\}.$$

Numerical scheme

Step 1: Solve the Cahn-Hilliard equation using a convex-splitting method: find $(\phi_h^{n+1}, \mu_h^{n+1}) \in W_h \times W_h$, such that for $\forall w_h \in W_h$,

$$\begin{cases} (\dfrac{\phi_h^{n+1} - \phi_h^n}{\delta t}, w_h) + (\mathbf{u}_h^n \cdot \nabla \phi_h^n, w_h) = -\mathcal{L}_d(\nabla \mu_h^{n+1}, \nabla w_h), \\ \\ (\mu_h^{n+1}, w_h) = \epsilon(\nabla \phi_h^{n+1}, \nabla w_h) + \dfrac{s}{\epsilon}(\phi_h^{n+1}, w_h) + \dfrac{1}{\epsilon}((\phi_h^n)^3 - (1+s)(\phi_h^n), w_h) \\ +\langle [\dfrac{1}{\mathcal{V}_s}(\dfrac{\phi_h^{n+1} - \phi_h^n}{\delta t} + u_{\tau_1,h}^n \partial_{\tau_1} \phi_h^n + u_{\tau_2,h}^n \partial_{\tau_2} \phi_h^n) - \dfrac{\sqrt{2}}{6}\pi \cos\theta_s^{surf} \cos(\dfrac{\pi}{2}\phi_h^n) \\ +\tilde{\alpha}(\phi_h^{n+1} - \phi_h^n)], w_h\rangle. \end{cases} \tag{3.1}$$

Step 2: Update ρ^{n+1}, η^{n+1} and l_s^{n+1}:

$$(\rho^{n+1}, \eta^{n+1}, l_s^{n+1}) = \frac{1+\phi^{n+1}}{2} + (\lambda_\rho, \lambda_\eta, \lambda_{l_s})\frac{1-\phi^{n+1}}{2}. \tag{3.2}$$

Numerical scheme

Step 3: Solve the velocity system of Navier-Stokes equations using a pressure stabilization scheme: find $\mathbf{u}_h^{n+1} \in \mathbf{U}_h$, such that for $\forall \mathbf{v}_h \in \mathbf{U}_h$,

$$\begin{aligned}
&\mathrm{Re}\left(\left[\frac{\frac{1}{2}(\rho^{n+1} + \rho^n)\mathbf{u}_h^{n+1} - \rho^n \mathbf{u}_h^n}{\delta t} + \rho^{n+1}(\mathbf{u}_h^n \cdot \nabla)\mathbf{u}_h^{n+1} + \frac{1}{2}(\nabla \cdot (\rho^{n+1}\mathbf{u}_h^n))\mathbf{u}_h^{n+1} \right], \mathbf{v}_h \right) \\
&= -(\eta^{n+1}(\nabla \mathbf{u}_h^{n+1} + (\nabla \mathbf{u}_h^{n+1})^T), \nabla \mathbf{v}_h) + \mathcal{B}(\mu_h^{n+1} \nabla \phi_h^{n+1}, \mathbf{v}_h) + (2p_h^n - p_h^{n-1}, \nabla \cdot \mathbf{v}_h) \\
&- \langle [\mathcal{L}_s(\phi_h^{n+1}) l_s]^{-1} (u_h^{n+1})_{\tau_1}^{slip}, v_{\tau_1,h} \rangle - \langle [\mathcal{L}_s(\phi_h^{n+1}) l_s]^{-1} (u_h^{n+1})_{\tau_2}^{slip}, v_{\tau_2,h} \rangle \\
&+ \mathcal{B}\langle (\partial_n \phi_h^{n+1} - \frac{\sqrt{2}}{6}\pi \cos\theta_s^{surf} \cos(\frac{\pi}{2}\phi_h^{n+1}) + \tilde{\alpha}(\phi_h^{n+1} - \phi_h^n))\partial_{\tau_1}\phi_h^{n+1}, v_{\tau_1,h} \rangle \\
&+ \mathcal{B}\langle (\partial_n \phi_h^{n+1} - \frac{\sqrt{2}}{6}\pi \cos\theta_s^{surf} \cos(\frac{\pi}{2}\phi_h^{n+1}) + \tilde{\alpha}(\phi_h^{n+1} - \phi_h^n))\partial_{\tau_2}\phi_h^{n+1}, v_{\tau_2,h} \rangle. \qquad (3.3)
\end{aligned}$$

Step 4: Solve the pressure system of Navier-Stokes equations: find $p_h^{n+1} \in W_h$, such that for $\forall q_h \in W_h$,

$$(\nabla(p_h^{n+1} - p_h^n), \nabla q_h) = -\frac{\bar{\rho}}{\delta t}\mathrm{Re}(\nabla \cdot \mathbf{u}_h^{n+1}, q_h), \qquad (3.4)$$

where $\bar{\rho} = \min(1, \lambda_\rho)$.

Outline

Domain decomposition methods

- MCL problem requires a very fine mesh to capture the interface, especially in 3D as $\epsilon \to 0$.
- Distributed computing based on MPI: reduces the compute time and provides necessary amount of memory.
- A partition of the domain $\Omega_h = \Omega_{h,1} \cup \cdots \cup \Omega_{h,np}$ where $\Omega_{h,i} \cap \Omega_{h,j} = \emptyset$ for all $i \neq j$.
- Meshes are partitioned using Metis on a relatively coarse level and are refined sufficiently for computation.

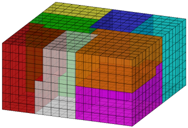

(a)

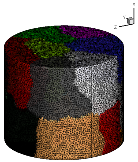

(b)

Figure: (a) A sample partition of a structured mesh into 8 subdomains and (b) a partition of an unstructured mesh into 16 subdomains.

Solution algorithms

$$A_h M_h^{-1} y_h = b_h, \text{ with } x_h = M_h^{-1} y_h, \tag{4.1}$$

- A geometrical restrict additive Schwarz (RAS) [Cai and Sarkis, 99] preconditioned GMRES method is employed to solve the implicit systems of (ϕ, μ) and $\mathbf{u}$.

$$b_{h,i}^{\delta} = R_{h,i}^{\delta} b_h = (I \quad 0) \begin{pmatrix} b_{h,i}^{\delta} \\ b \backslash b_{h,i}^{\delta} \end{pmatrix},$$

$$M_h^{-1} = \sum_{i=1}^{np} (R_{h,i}^{0})^T (A_{h,i})^{-1} R_{h,i}^{\delta},$$

$$A_{h,i} = R_{h,i}^{\delta} A_h (R_{h,i}^{\delta})^T.$$

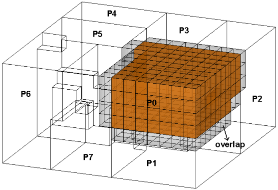

- An algebraic multigrid (AMG) preconditioned CG method is used to solve the pressure Poisson system.
  — BoomerAMG from Hypre library is used,
  — HMIS coarsening, multipass interpolation, and a hybrid SOR/Jacobi smoother.

Outline

Parallel Software Development

- Unstructured meshes are generated with **Gmsh** and partitioned with **Metis**.
- FEM implementation is realized by using **Libmesh**.
- Parallel solver is implemented using **PETSc**.
- Computations are carried out on the **Tianhe2 Supercomputer** (Rank 1st in Top500) in Guangzhou, China.

Cavity flow with shear velocity

A moving contact line problem of a cavity flow with shear velocity $\mathbf{u}_w = (0, \pm 0.4, 0)$ imposed on the top and bottom boundaries.

- $\Omega = (-0.05, 0.05) \times (-0.1, 0.1) \times (-0.1, 0.1)$
- Element pair: Q1-Q1, $\delta t = 0.05h$

$$\lambda_\rho = 0.1, \quad \lambda_\eta = 0.2, \quad \lambda_{l_s} = 10, \quad \mathrm{Re} = 10, \quad \theta_s^{surf} = 77.6^\circ, \quad \epsilon = 0.01,$$
$$\mathcal{L}_d = 5.0 \times 10^{-4}, \quad \mathcal{B} = 40, \quad \mathcal{V}_s = 500, \quad l_s = 0.0038, \quad s = 1.5, \quad \alpha = 0.125.$$

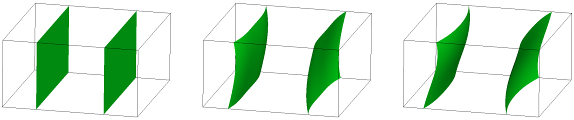

(a) (b) (c)

Figure: A cavity flow of two fluids driven by a shear velocity $(0, \pm 0.4, 0)$ on top and bottom boundaries. The evolution of the interface is shown at time steps (a) 0, (b) 500, and (c) 2,000.

Droplet impact on rough surface

We consider the impact of a droplet towards a rough solid surface, with initially downward momentum. The computational domain of this case is $\Omega = (0.025\mathrm{Sin}(x), 1.2) \times (-0.025\pi, 0.5\pi) \times (0, 0.5\pi)$, $x \in (-\pi, 20\pi)$. A spherical drop is initially located at $(0.35, 0.2375\pi, 0.25\pi)$ with radius 0.3 and initial speed $(-1, 0, 0)$.

$$\lambda_\rho = 0.001, \quad \lambda_\eta = 0.1, \quad \lambda_{l_s} = 1, \quad \mathrm{Re} = 1000, \quad \theta_s^{surf} = 50^\circ, \quad \epsilon = 0.02,$$
$$\mathcal{L}_d = 5.0 \times 10^{-4}, \quad \mathcal{B} = 12, \quad \mathcal{V}_s = 500, \quad l_s = 0.038, \quad s = 1.5, \quad \alpha = 0.374.$$

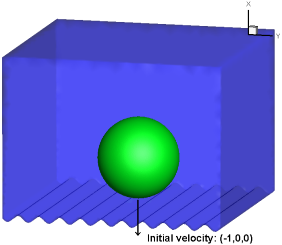

(a)

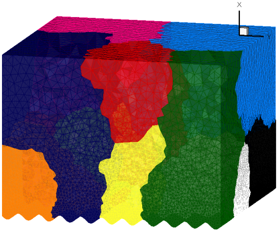

(b)

Figure: (a) Initial condition and (b) a sample partition into 16 subdomains for the droplet spreading case. The mesh has 3,437,991 elements and 535,509 vertices.

Droplet impact on surface boundary

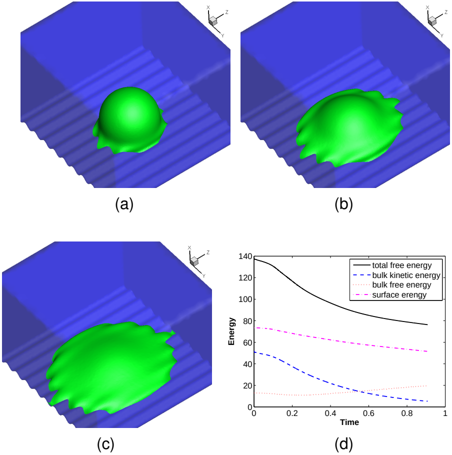

Figure: Droplet spreading on a rough surface. The interface is shown at times (a) $t = 0.2$, (b) $t = 0.4$, and (c) $t = 0.6$. Four energy terms as functions of time are shown in (d).

A bumpy channel flow of two fluids

Flow of two immiscible fluids in a bumpy channel driven by the pressure gradient. The computational domain of this case is $[-0.5, 0.5] \times [-0.075, 0.075] \times [-0.075, 0.075]$. By this simulation we investigate the influence of interfacial tension and wettability by changing the contact angle.

$$\lambda_\rho = 0.8, \quad \lambda_\eta = 2, \quad \lambda_{l_s} = 1, \quad \mathrm{Re} = 5, \quad \epsilon = 0.005, \quad \mathcal{L}_d = 5.0 \times 10^{-4},$$
$$\mathcal{B} = 12, \quad \mathcal{V}_s = 200, \quad l_s = 0.0025, \quad s = 1.5, \quad \alpha = 0.125, \quad \delta t = 0.05h.$$

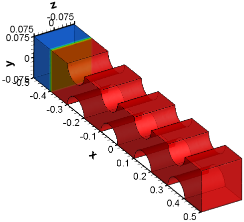

(a)

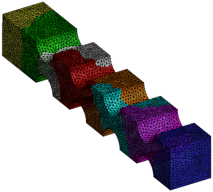

(b)

Figure: (a) Initial condition and (b) a sample partition into 8 subdomains for the channel flow case. The mesh has 662,283 elements and 113,457 vertices.

A bumpy channel flow of two fluids

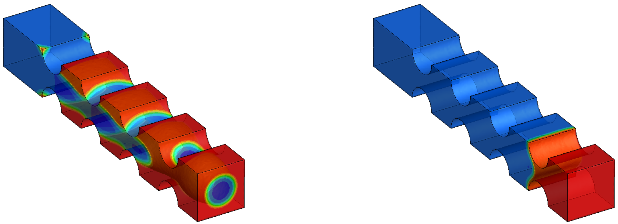

(a) (b)

Figure: Dynamics of the interface in a bumpy channel at $t = 1.3$ with contact angle (a) $\theta_s^{surf} = 120^\circ$ and (b) $\theta_s^{surf} = 60^\circ$.

Dropped particle across a fluid-fluid interface

A solid particle is dropped across a fluid-fluid interface.

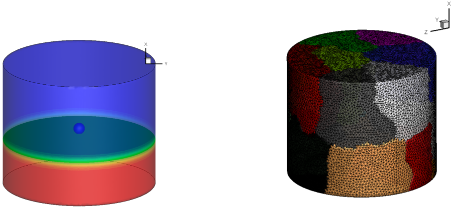

(a) (b)

Figure: (a) Initial condition and (b) a sample partition of an unstructured mesh into 16 subdomains. The mesh has 406,597 elements and 73,417 vertices.

$$\lambda_\rho = 0.1, \quad \lambda_\eta = 0.1, \quad \lambda_{l_s} = 1, \quad \mathrm{Re} = 100,$$
$$\mathcal{B} = 12, \quad Fr = 0.032, \quad \rho_p = 1000, \quad r_p = 0.015,$$
$$\mathcal{L}_d = 5.0 \times 10^{-4}, \quad \mathcal{V}_s = 500, \quad l_s = 0.0025, \quad \epsilon = 0.01.$$

Movies

Figure: Dynamic process of ϕ for case (left) $\theta^{surf} = 60^\circ$, (right) $\theta^{surf} = 150^\circ$.

Outline

Parallel performance

The cavity flow case with 67,108,864 elements and 67,634,433 vertices: the impact of overlap in the Schwarz preconditioner for solving the Cahn-Hilliard system and the velocity system. ILU(1) is used as the subdomain solver.

Table: A strong scalability test for the cavity flow case. The average number of GMRES iterations, compute time per time step, speed up, and efficiency for solving Cahn-Hilliard system and the velocity system.

		Cahn-Hilliard system #unknowns=135,268,866				velocity system #unknowns=202,903,299			
np	overlap	GMRES	time	sp.	eff.	GMRES	time	sp.	eff.
3,840	0	30.5	2.30	1	100%	27.2	8.34	1	100%
3,840	1	19.3	2.09	1	100%	17.2	9.34	1	100%
5,760	0	31.6	1.70	1.35	90%	28	5.80	1.48	98.6%
5,760	1	19.8	1.58	1.32	88%	17.7	7.01	1.33	88.7%
7,680	0	31.9	1.51	1.52	76%	28.5	5.23	1.59	79.5%
7,680	1	19.8	1.39	1.50	75%	17.7	6.16	1.52	76%
9,600	0	31.9	1.18	1.95	78%	28.4	3.81	2.19	87.6%
9,600	1	19.8	1.10	1.90	76%	17.7	4.39	2.13	85.2%

- The numbers of GMRES iterations stay near constants.
- When with overlap, the numbers of GMRES iterations are reduced by roughly $1/3$, leading to the reduction of time for the Cahn-Hilliard solver, but the growth of time for the velocity solver.

Parallel performance

The cavity flow case with 67,108,864 elements and 67,634,433 vertices

Table: A strong scalability test for the cavity flow case. The average number of CG iterations, compute time per time step, speed up, and efficiency for solving the pressure system. The number of sweeps in the multigrid preconditioner is fixed to 2

pressure system #unknowns=67,634,433				
np	CG	time	sp.	eff.
3,840	16.3	1.61	1	100%
5,760	17.5	1.29	1.25	83.2%
7,680	18.2	1.21	1.33	66.5%
9,600	17.4	0.94	1.71	68.5%

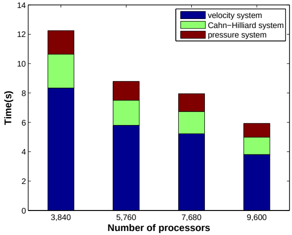

Figure: Distribution of compute time for the cavity flow case.

- A moderate performance with efficiency 68.5% is observed for the pressure solver.
- Most of the compute time is spent on the velocity solver.

Parallel performance

The channel flow case with 344,460,747 elements and 51,270,353 vertices: different levels of ILU fill-ins in the Schwarz preconditioner for solving the Cahn-Hilliard system and the velocity system. The overlap size is fixed to 1.

Table: A strong scalability test for the channel flow case. The average number of GMRES iterations, compute time per time step, speed up, and efficiency for solving Cahn-Hilliard system and the velocity system.

		Cahn-Hilliard system #unknowns=102,540,706				velocity system #unknowns=153,811,059			
np	subsolve	GMRES	time	sp.	eff.	GMRES	time	sp.	eff.
1,920	ILU(1)	441.4	21.36	1	100%	35	13.72	1	100%
1,920	ILU(2)	39.9	4.36	1	100%	13.7	17.18	1	100%
1,920	ILU(3)	12.7	3.60	1	100%	6.8	25.61	1	100%
5,760	ILU(1)	-	-	-	-	30	4.57	3.00	100%
5,760	ILU(2)	42.2	1.80	2.42	80.7%	13.1	6.06	2.83	94.5%
5,760	ILU(3)	13.4	1.43	2.52	84%	7	9.38	2.73	91%
9,600	ILU(1)	-	-	-	-	29.8	3.38	4.06	81.2%
9,600	ILU(2)	40.6	1.29	3.38	67.6%	14.3	4.27	4.02	80.5%
9,600	ILU(3)	13.7	1.09	3.30	66%	9.8	6.63	3.86	77.3%

- ILU(1) does not work for the Cahn-Hilliard system on 5,760, and 9,600 processors.
- Increasing the level of fill-ins helps reduce the number of GMRES iterations.
- ILU(3) is the best choice for the Cahn-Hilliard system and ILU(1) is the best choice for the velocity system.

Parallel performance

The channel flow case with 344,460,747 elements and 51,270,353 vertices: varying the number of sweeps of the smoother in the multigrid preconditioner for solving the pressure system.

Table: A strong scalability test for the channel flow case. The average number of CG iterations, compute time per time step, speed up, and efficiency for solving the pressure system.

pressure system #unknowns=51,270,353					
np	sweep	CG	time	sp.	eff.
1,920	1	24.1	2.74	1	100%
1,920	2	20.2	3.31	1	100%
1,920	3	19.8	3.92	1	100%
5,760	1	24.1	1.15	2.38	79.4%
5,760	2	20.7	1.42	1.63	54.2%
5,760	3	19.7	1.66	2.36	78.7%
9,600	1	24.8	0.95	2.88	57.7%
9,600	2	21	1.13	2.92	58.6%
9,600	3	19.9	1.34	2.93	58.5%

- The number of CG iterations remains to be independent of *np*.
- One sweep of smoother is preferable for the AMG method.

Parallel performance

The channel flow case with 344,460,747 elements and 51,270,353 vertices: combine the above choices to the solution algorithm, we present the speedups and compute time for each system.

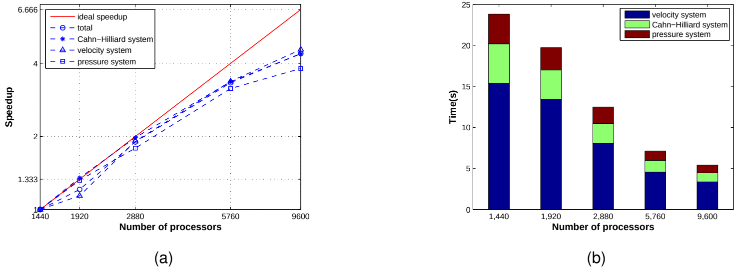

Figure: (a) Speedups and (b) distribution of compute time for the solutions of the channel flow case.

- Nearly excellent speedup is achieved when *np* trends to 2,880 and a final speedup of the whole solution is 4.39 for this test.

Outline

Summary

- A phase-field model with GNBC was discretized by a semi-implicit scheme in time and a finite element method in space.
- A newly developed parallel finite element solver and its implementation on a parallel computer.
- Numerical tests are carried out to verify the effectiveness of the scheme.
- The results of two strong scalability tests indicate that the solution algorithm has a good speedup on both structured and unstructured meshes.

Thank You